SPIRE

Calculation of Important Parameters for SPIRE Scan Map Observations

Prepared by: **Tim Waskett**
Bruce Sibthorpe

Document number: **SPIRE-UCF-NOT-002884**

Issue: **1.0** **Date:** **01 May 2007**

Contents

1. Introduction

This is a brief note to describe how to calculate various parameters that are important for properly implementing SPIRE scan map mode. These parameters include the ***effective integration time*** for a SPIRE scan map observation, as well as the ***scan direction, scan leg separation*** distance and the ***map size*** that results from a particular scan pattern. Please excuse the random order in which these are dealt with; it should all become clear when read as a whole.

2. Effective Integration Time

The effective integration time is how long the SPIRE array spends observing any given point of the sky during a scan map observation. This is a distinctly different quantity to the total observing time, which is the entire length of time it takes to observe the whole map. The effective integration time, per map repeat, is only dependent on the scan rate of the arrays across the sky, as shall be shown later. This quantity does not increase if the map is made bigger but will increase if the same area of sky is observed again by subsequent map repeats.

Imagine a single point source that lies in the path of a SPIRE scan map observation. The arrays head straight towards it at the scan speed *v*, assumed to be 30"/s in a nominal observation. The edge of the array arrives at the source and the effective integration time on that source begins to increase (part 1 in Figure 1). The arrays continue across the source until the far edge of the array passes over the source and the arrays head off into the distance (part 2). At this point the effective integration time stops increasing and the source will not be observed again during the rest of that map repeat, no matter how large the final map will become. This is because subsequent scan legs will move the arrays far enough away from the source that it will not be passed over again. Sources that lie in the path of the array corner, for example, will ultimately have the same effective integration time as the source in this example because the source *will* be observed a second time by a subsequent scan leg.

So, a simple way of calculating the effective integration time is to calculate the time it takes for the SPIRE arrays to pass over a point on the sky. I.e. it will be the width or length of the arrays in the scan direction (the red lines in the following schematic), divided by the scan rate, *v*.

Figure 1. Schematic showing how effective integration time can be visualised.

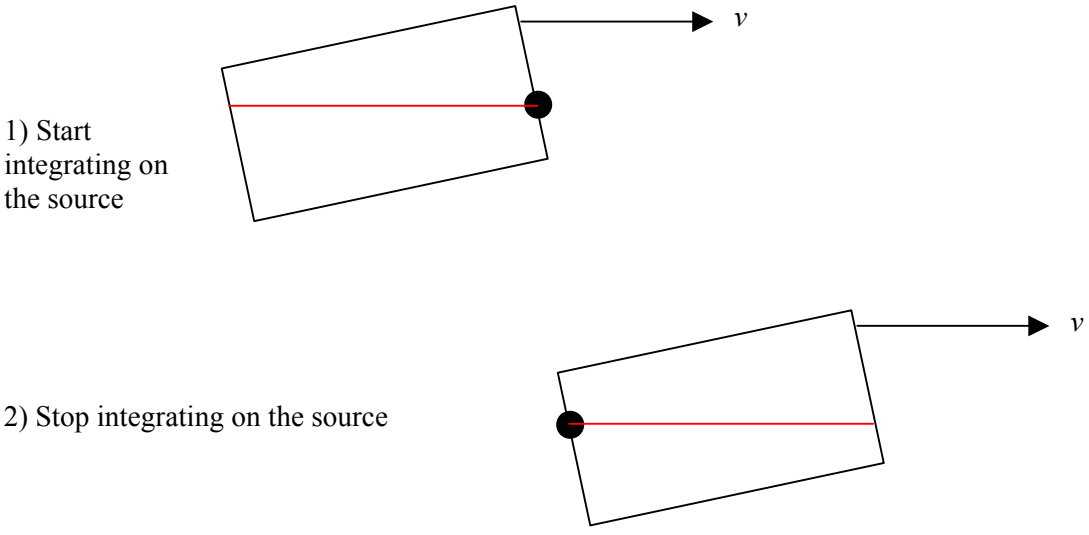

In fact, this calculation gives identical results to using the method described in section 5 of [1].

3. Geometry

Figure 2 shows a schematic demonstrating how the scan leg separation and the effective integration time can be calculated by considering how a scan map is built up, for a diagonal scan direction (the same principle applies to the other two scan directions.) The green rectangles show the effective area of the PSW array and how it relates to the feedhorns. Imagine placing many of these rectangles together so that there is no space

between them and so that the feedhorns of adjacent arrays fit neatly beside each other. This is effectively the arrangement we are looking for when we perform a scan map. It is as if one enormous array has scanned across the sky and not one array passing back and forth many times, as is the reality. You will now see how the green rectangle has been defined. I define the scan leg separation with respect to this PSW rectangle because it is the smallest of the three arrays. The PMW and PLW arrays can have similar rectangles defined but they are larger because the detectors are physically larger, which means that there are regions of extra overlap in scan maps for these two arrays, which is obviously no bad thing.

Figure 2. Schematic showing how various scan map parameters can be derived from simple geometric arguments.

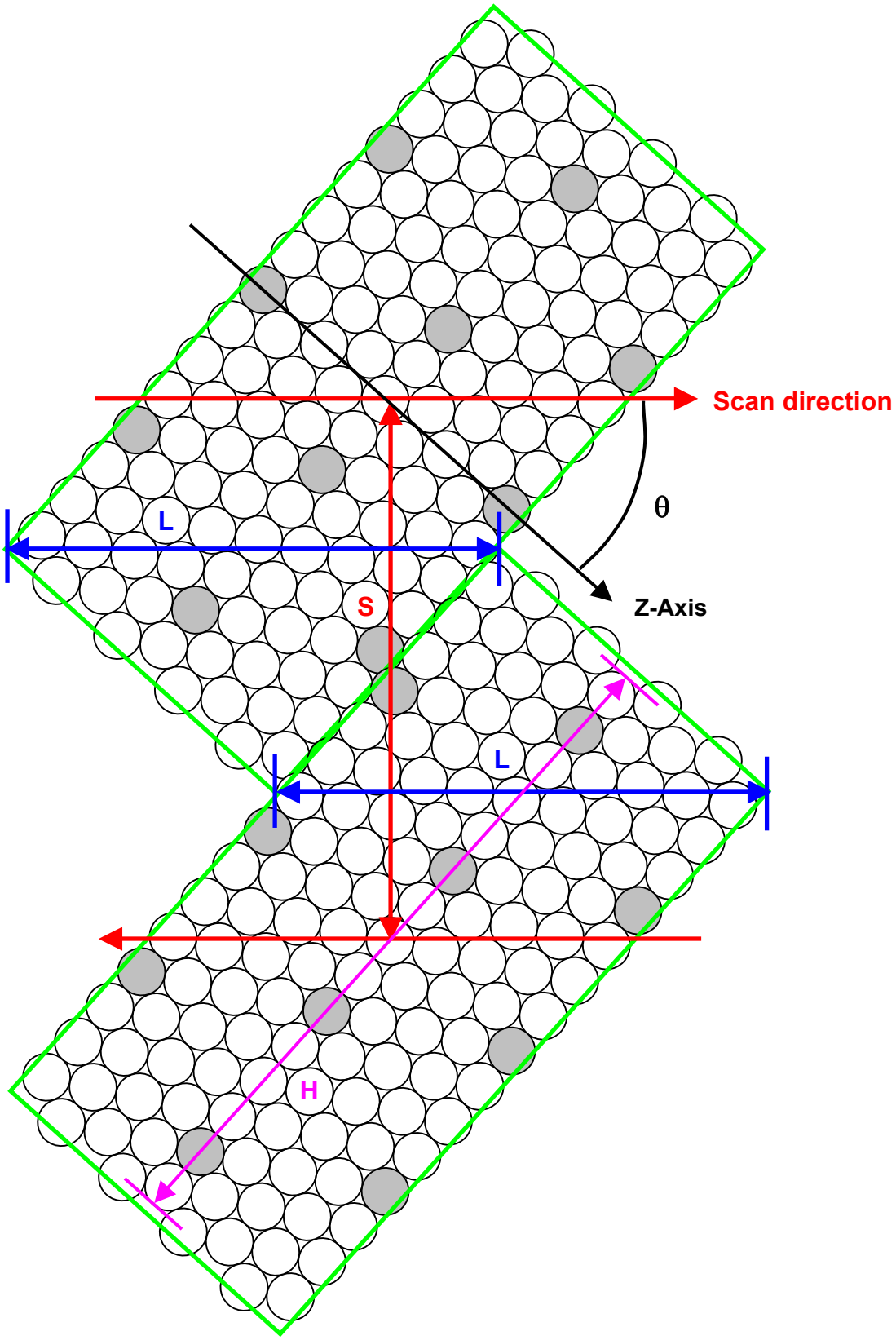

The array length in the scan direction (**L**) can be calculated quite simply from the size of the green rectangle and it's rotation with respect to the Z-axis, **θ**. In this example **θ** = 42.4° and the array width in the Z direction is 244.7" (the width of the array in the Z direction = 31.4*0.5*9√3 = 244.7", where the detector spacing is 31.4", there are 9 rows of detectors and the spacing between the rows is 0.5*√3 times the detector spacing), so:

$$L = \frac{244.7}{\cos(\theta)} = 331.1"$$

The scan leg separation, **S**, can be derived in a similar way. In this case, see how the corners of the two rectangles are aligned in the scan direction, to either side of the blue arrows, so that once both scan legs are complete the map area in the overlap region has been crossed by as many detectors as the rest of the map, i.e. if you took a vertical slice through the middle of the map the integration time is the same at all points, because **L** is constant (except for the extreme top and bottom corners, which taper to a point and hence **L** tends to zero.) The separation, **S**, is just the length of one green rectangle in the cross-scan (i.e. vertical) direction (or the array centre-to-centre spacing, as indicated by the red vertical arrow), so:

$$S = \frac{244.7}{\sin(\theta)} = 363"$$

Figure 3. Alternative way of calculating scan leg separation distance.

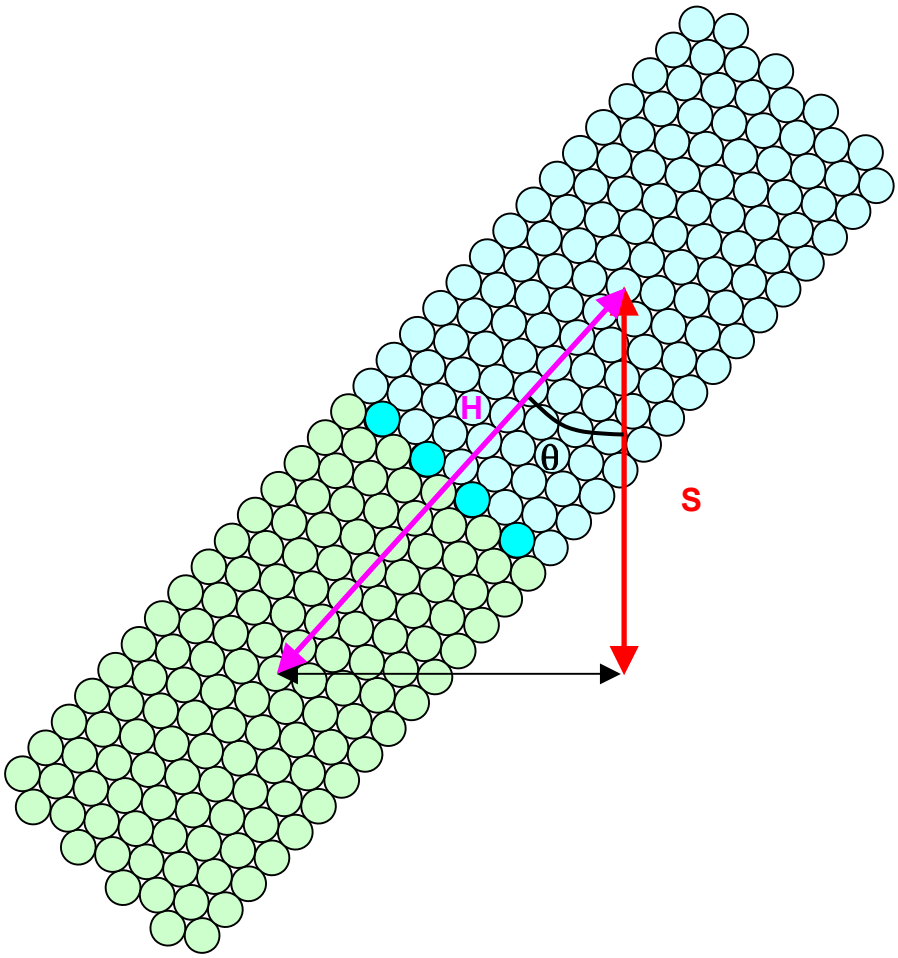

However, there is an alternative way of calculating **S** that ensures a slightly more robust coverage in the overlap region, providing a small degree of extra redundancy, just in case. This is defined by considering the magenta line in Figure 2 and Figure 3, labelled as **H**. By using this distance to define the array size, rather than the length of the green rectangle, we are effectively overlapping the four detectors at each end of the PSW array; the heavily shaded ones in Figure 3. This has the advantage that there are four strips of data with double redundancy in the final map. To calculate **S** from **H** is just as simple, assuming that we know the detector spacing for the PSW array, which is 31.4":

$$H = 31.4 \times 15 = 471"$$

$$S = H \times \cos(\theta) = 348"$$

I prefer this value for the separation due to the extra redundancy, but any value between 348" and 363", for diagonal scanning, would be just fine. Equivalent values can be derived for the short scanning direction (449 – 455"), but for long axis scanning the geometry is more complicated and to ensure uniform coverage the value of 235" was found to be the most satisfactory separation, as calculated from the following equation (please don't ask me to explain where this equation comes from, it's a nightmare):

$$S_{long} = \frac{31.4 \times 9\sqrt{3}}{2}\sin(77.6) - \frac{31.4}{2}\cos(77.6) = 235"$$

All these separations have been verified by simulated observations.

Table 1 defines the dimensions of the three array sizes in the same way as the green rectangles in Figure 2. The array heights (long axis) are calculated by assuming a half integer number of detectors, i.e. the average number between two adjacent rows.

Table 1. Array sizes defined by the green rectangle in Figure 2. All dimensions are in arc seconds.

Array	Height	Width	Detector spacing
PSW	486.7	244.7	31.4
PMW	522.5	253.4	41.8
PLW	533.8	271.9	62.8

4. Some Numbers

Table 2 shows the effective integration times calculated for the three arrays and for the three possible scan angles, using the array sizes defined in Table 1, i.e. **L**/*v*. These integration times refer to a *single map repeat.* The total effective integration time for an observation with multiple map repeats is simply this number multiplied by the number of map repeats. The different arrays have different effective integration times because they actually cover slightly different areas of the sky. These numbers have all been verified by the SPIRE Photometer Simulator to within 2%, using the alternative method described in section 5 of [1].

Table 2. summary of the effective integration times for the three SPIRE arrays and for the three allowed scan directions. *v* is the scan speed in "/s, giving effective integration times per map repeat in seconds.

Array	Short	Diagonal	Long
PSW	257/*v* = 8.57 s	331/*v* = 11.03 s	498/*v* = 16.60 s
PMW	266/*v* = 8.87 s	343/*v* = 11.43 s	535/*v* = 17.83 s
PLW	285/*v* = 9.50 s	368/*v* = 12.27 s	547/*v* = 18.20 s

These numbers are entirely general for any scan speed, as indicated, but the specific example given in the table is for a scan speed of 30"/s. It is no surprise that the effective integration time for long axis scanning is about twice that for short axis scanning; the array is roughly twice as long as it is wide.

Caveat: These effective integration times do not include the effects of vignetting, so for the PMW and PLW arrays a small correction may need to be included. However, since the scan leg separations are

calculated for the slightly smaller PSW array, the extra overlap experienced by the other two arrays may be enough to offset the effects of vignetting.

5. Effective Integration Time for PACS-SPIRE Parallel Mode – pMode

pMode sensitivity is slightly different to that for normal SPIRE scanning because the scan leg separation distance is not the same as for SPIRE only scanning. pMode uses the diagonal scan direction and a separation of 155" rather than the 348" used for SPIRE only diagonal scanning. This increases the effective integration time of the SPIRE observation because each point on the sky is observed more than once by the SPIRE arrays.

A simple conversion from SPIRE only scanning to pMode can be achieved by multiplying the effective integration time by the ratio of the separations:

$$\tau_{eff}(pMode) = \tau_{eff}(SPIRE)\frac{Sep(SPIRE)}{Sep(pMode)}$$

So, for the case of the nominal pMode, using diagonal scanning, the effective integration time for the three arrays are as follows:

Array	τ_{eff}
PSW	743/v
PMW	770/v
PLW	826/v

The method described in section 5 of [1] provides slightly different values for the PMW and PLW arrays (11% higher for PMW, 15% higher for PLW) because the SPIRE only separation is optimised for the slightly smaller PSW array, meaning that extra integration time exists in the overlap region for the other two arrays. This extra time is not included in Table 2 because it only applies to the small overlap region and is not indicative of the majority of the map. I choose to disregard it here too to retain consistency and to err on the side of caution. Also, vignetting may counteract this extra overlap, so in reality these numbers are probably quite close to the true value across the whole map.

6. Sensitivity

The effective integration time can be used to convert the $\Delta S\_1\sigma\_1s$ value into a sensitivity per map repeat in the usual way:

$$\Delta S\_1\sigma = \frac{\Delta S\_1\sigma\_1s}{\tau_{eff}^{0.5}}$$

Where τ_{eff} is the effective integration time.

6.1 Sensitivity for Combined Observations

It is possible that more than one observation will need to be combined to integrate to a particular sensitivity. For example, a nominal scan direction may need to be combined with an orthogonal scan direction. In this case the final sensitivity will be determined by the total sum of the effective integration times for all the separate components added together. Once the total τ_{eff} is found then the final sensitivity can be calculated using the formula above. I shall provide a few examples here for clarification.

Example 1: PSW sensitivity. Diagonal scanning, two map repeats each of the nominal and orthogonal scan directions.

τ_{eff}(total) = 2*331/v + 2*331/v = 4*331/v

Example 2: PSW sensitivity. 2 repeats of a long axis observation plus 4 repeats of a short axis observation.

τ_{eff}(total) = 2*498/v + 4*257/v = 2024/v

In General this can be summarised by the following formula:

$$\tau_{eff}(total) = \sum_i \left(N^i \cdot \tau_{eff}{}^i \right)$$

Where τ_{eff}^i are the effective integration times per map repeat for the different layers, found in Table 2.

The final sensitivity is given by:

$$\Delta S\_1\sigma = \frac{\Delta S\_1\sigma\_1s}{\tau_{eff}(total)^{0.5}}$$

Things are further complicated by using different scan speed for different observations but in this case the only care that needs to be taken is to incorporate the scan speed in the calculation of the individual τ_{eff}^i values before combining them together with the relevant number of map repeats.

7. Scan Direction

I have already mentioned the scan direction (θ) above but now I shall justify the particular choice of angle and its derivation. Certain members of the SPIRE instrument team disagree with the current nominal scanning angle so I shall present the two arguments and the pros and cons for each.

For simplicity I shall briefly redefine θ as the angle through which the SPIRE arrays must be rotated **with respect to one of the three symmetry axes**. This is an important distinction as usually angles are defined with respect to the Z-axis of the array, which is actually not one of the symmetry axes. The Y-axis is a symmetry axis, however, as are rotations of 60° about the Y-axis. See [3] for some helpful diagrams illustrating the various angles, as well as further arguments for both angles presented here.

The two angles under consideration here are as follows:
Double Nyquist angle $\theta = 12.4°$ (Figure 4)
Nyquist angle $\theta = 13.9°$ (Figure 5)

My preference is for the Double Nyquist angle, which when combined with the symmetry axis that is 60° around from the Y-axis, gives a scan direction of 42.4° w.r.t. the Z-axis of the arrays.

Figure 4. Double Nyquist scan angle along the diagonal direction (42.4° relative to the Z-axis.) The red arrows indicate the path of each detector in the array, the black arrow is a symmetry axis (the other two are not shown but would be 60° rotated with respect to this one), and the blue and green arrows are spacers indicating the same lines as shown in Figure 6. The Large circles show the physical size of the detector feedhorns while the smaller circles, both inside and outside of the array, show the size of the beam FWHM.

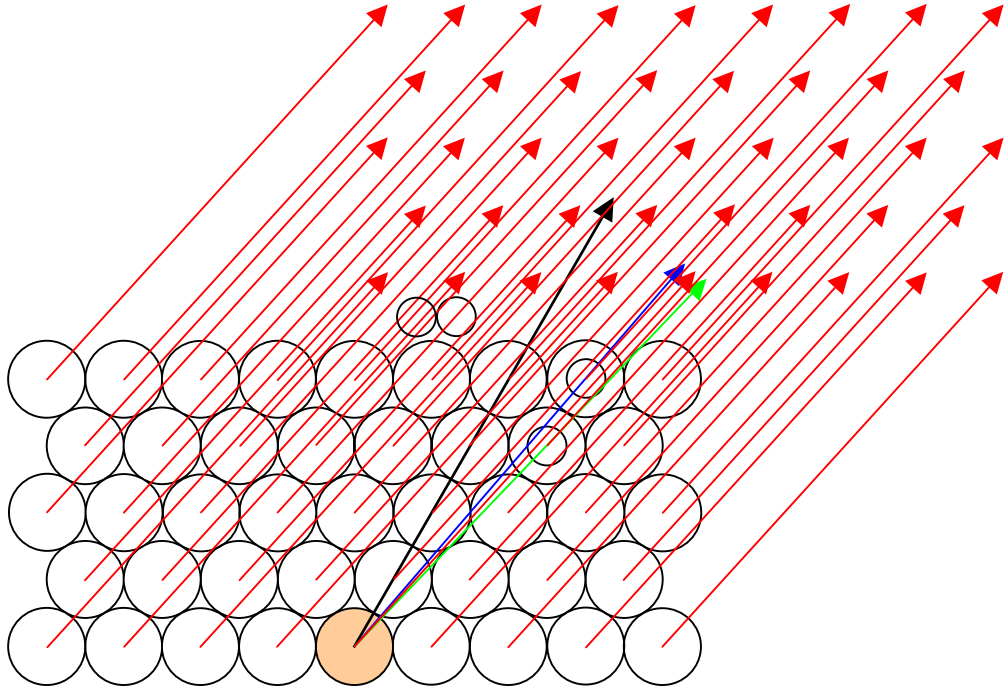

Figure 5. Nyquist scan angle along the diagonal direction (43.9° relative to the Z-axis.) The green arrows are now the path of the detectors, and in this case they follow the direction of the green arrows shown in Figure 4 and Figure 6, i.e. the path of the peach detector at the bottom of the array passes directly through the lower of the two detectors containing the small circles.

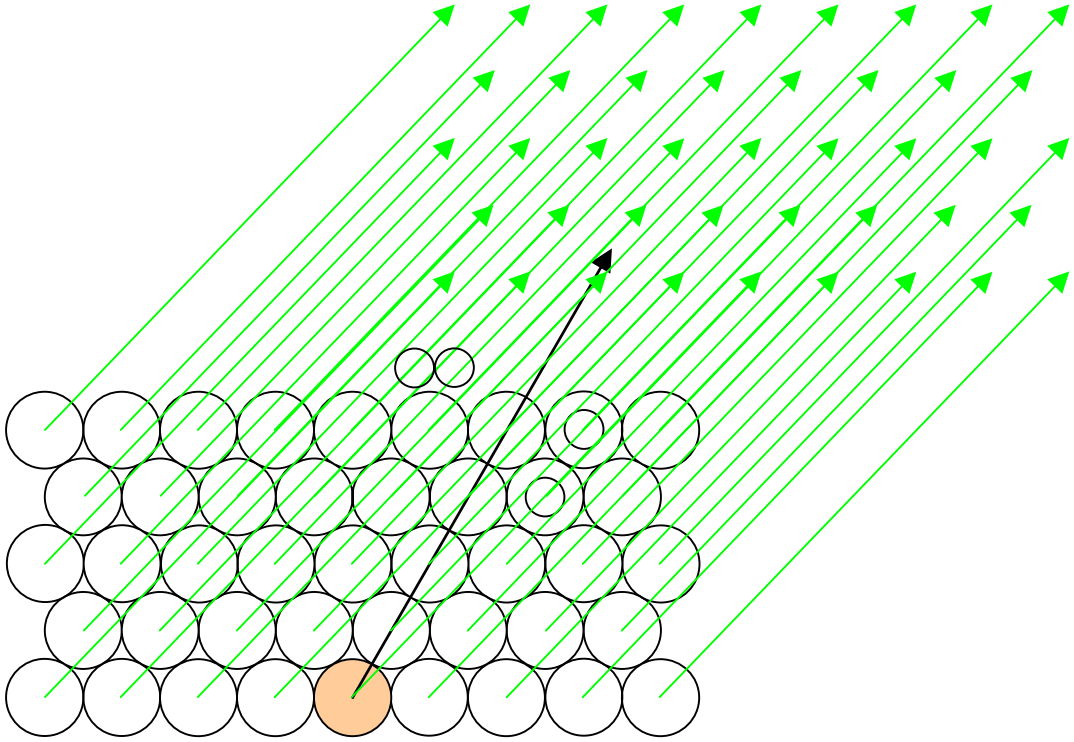

Nyquist sampling is defined so that the spacing between any two adjacent data points in a map is no more than half of a beam FWHM. This can be achieved by aiming the path of a detector exactly at another detector, as shown by the green line in Figure 6, joining the peach and green detectors (this geometry

provides the limiting case of just satisfying Nyquist sampling, see the equation later.) Inspecting Figure 6 it can be seen that this arrangement defines a triangle with 3.5 detectors along a symmetry axis and one detector to the side. In Figure 6 the symmetry axis in question is shown by the black arrow, while the first detector is indicated by the peach coloured shading. The green arrow shows the direction along which the array has to be scanned so that the path of the peach detector exactly overlaps with the green detector in order to achieve Nyquist sampling. Figure 5 shows what this looks like when the path of every PLW detector is plotted. The scan angle with respect to the symmetry axis is defined by:

$$\theta_N = \arctan\left(\frac{\sqrt{3}}{7}\right) = 13.9°$$

(The right-angle triangle, in Figure 6, defined by the symmetry axis and the scan direction has an opposite length of √3/2 and an adjacent length of 3.5.) And the distance between adjacent detector paths works out as:

$$d = s \cdot \sin(13.9°) = 0.24 \cdot s = 0.48 \cdot FWHM$$

where s is the detector centre-centre spacing. The strict definition of Nyquist sampling requires one data sample for every 0.5 FWHM for the beam to be fully sampled, so this scan angle comfortably satisfies the requirement of full beam sampling. The beam FWHM is indicated in Figure 4, Figure 5 & Figure 6 by the smaller circles.

Figure 6. Schematic showing the various angles described in the text.

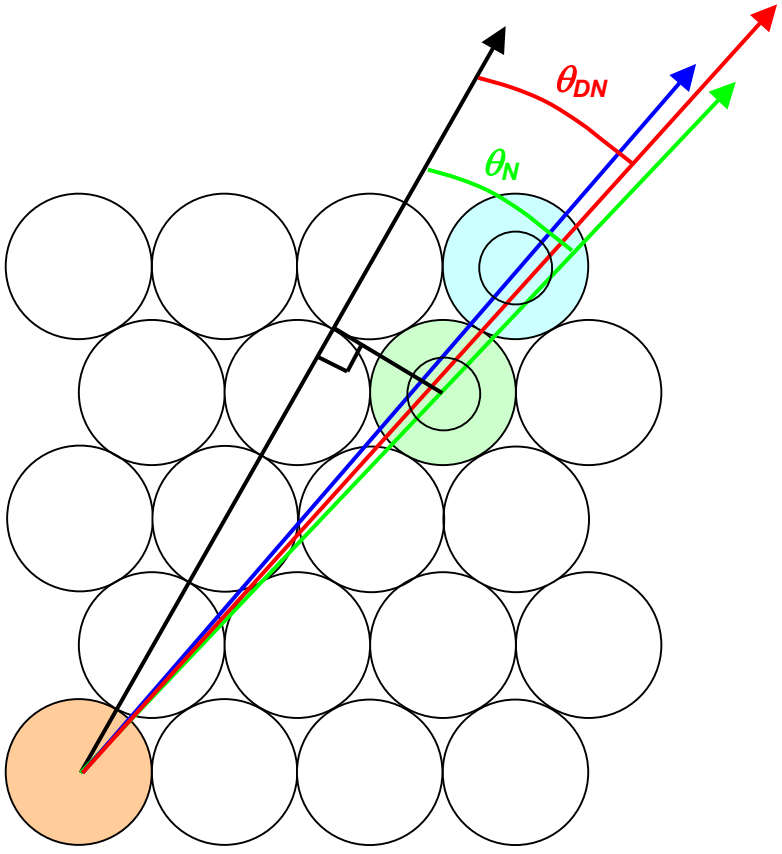

Double Nyquist sampling is defined so that the path of the peach detector passes exactly halfway between the centres of the blue and green detectors in Figure 6. The red arrow bisects the angle between the green and blue arrows to demonstrate this path. Figure 4 shows what this looks like when all the detector paths are plotted for the PLW array. The scan angle with respect to the symmetry axis is calculated as follows:

$$\theta_{DN} = 0.5 \cdot \left[\arctan\left(\frac{\sqrt{3}}{7}\right) + \arctan\left(\frac{\sqrt{3}}{9}\right) \right] = 12.4°$$

i.e. halfway between the green and the blue arrows = the red arrow.

As can be seen in Figure 4 the spacing between adjacent detector paths is now much smaller, for the most part. Pay particular attention to the two small circles just above the array itself to see how the beam FWHM is sampled for the PLW array. You will notice that the spacing is not entirely uniform as there are some gaps. This is only the case for the PLW array, whereas for the PMW and PSW arrays there are no gaps. The spacing between the detector paths works out at:

$$d = 0.5 \cdot s \cdot \sin(12.4°) = 0.107 \cdot s = 0.215 \cdot FWHM$$

For the PSW and PMW arrays the beam FWHM is being sampled with over double the frequency of Nyquist sampling across the whole map. The PLW map will be mostly sampled at this same high frequency but where there are gaps in the PLW coverage the spacing between adjacent detector paths is 0.43 FWHM, which is still better than with Nyquist sampling.

Compare Figure 4 and Figure 5 to see how this small change in angle completely changes the coverage of data across a scan map.

7.1 Pros and Cons

My preference for the Double Nyquist sampling angle is down to uniformity of map coverage. Not only is the beam sampled many times, allowing accurate sky reconstruction, but the coverage of data from one part of the map to another is much more uniform than with Nyquist sampling. See [3] for some interesting integration time maps similar to those shown in section 8. The gaps in coverage for the PLW array are still smaller than the spacing between detector paths for Nyquist sampling, so the sky is still better sampled and the coverage is still more uniform.

Nyquist sampling has one main advantage over Double Nyquist sampling; data redundancy. Because the path of one detector is scanned again by another detector, this information could be used to remove thermal drifts from the detector timelines on the time scale of a few seconds (the time it takes for the paths of the two detectors to overlap) to allow better sky reconstruction. However, thermal drifts should be dealt with pretty effectively by the data pipeline and by the mapmaking process (assuming cross-linked observations have been performed) so the benefit of this short timescale redundancy is not entirely clear. In my opinion the clear advantages offered by a more uniform sky coverage outweighs the potential benefits of this data redundancy.

Both angles are equally affected by missing detectors but by performing cross-linked observations any gaps in one map should be filled in by data from the orthogonal map.

At the time of writing, Double Nyquist sampling along the diagonal direction was the default scan strategy. Come flight time, if it is deemed that Nyquist sampling is the better bet, along any of the three directions (long, diagonal or short), then the information provided in this note should allow adjustment of the other parameters (map size, scan leg separation, effective integration time.)

8. Notes on Map Area Calculation

This section contains material first presented in [2]. It is repeated here for completeness.

When producing a large map, made up of many scan legs, the separation distance between subsequent scan legs is dependent on the scanning angle selected. These can be summarised as follows:

Scan Angle w.r.t. short (Z-) axis (deg)	Scan leg separation (arc sec)
+/- 77.6 (long)	235
+/- 42.4 (diagonal)	348
+/- 17.6 (short)	449

These separations ensure that the sky coverage of a large map is as uniform as possible. Because the PSW array has the smallest detectors these scan leg separations provide optimum sky coverage for the PSW but a slight excess of coverage in the overlap region for the other two arrays. The following integration time maps show examples of these separations for the PSW array (turn around data not included) – the darker the shading the greater the integration time. The red lines passing through the centre of the arrays show the scan legs and how they are separated.

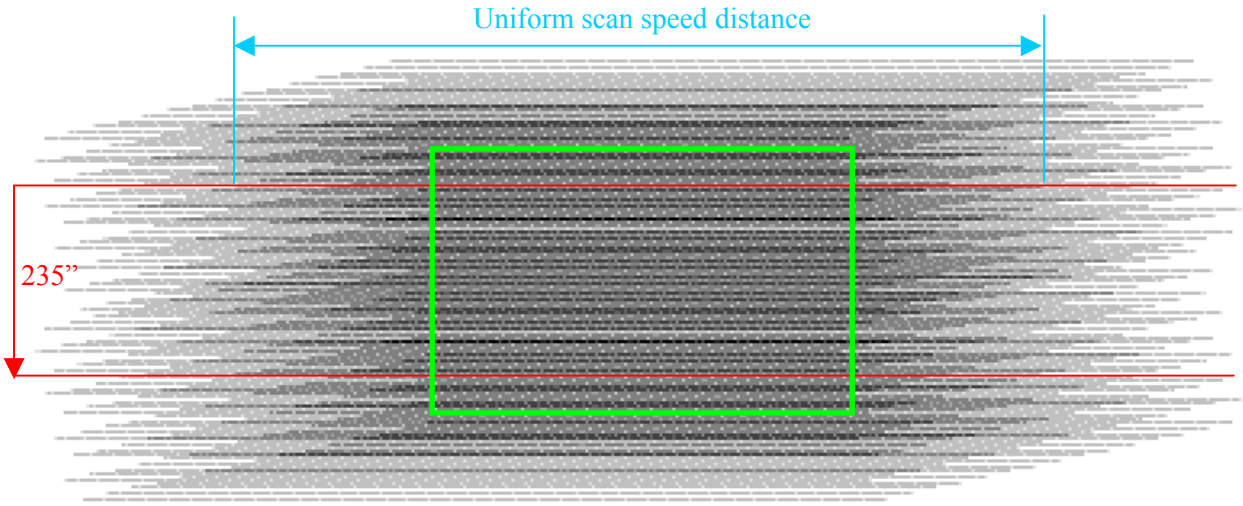

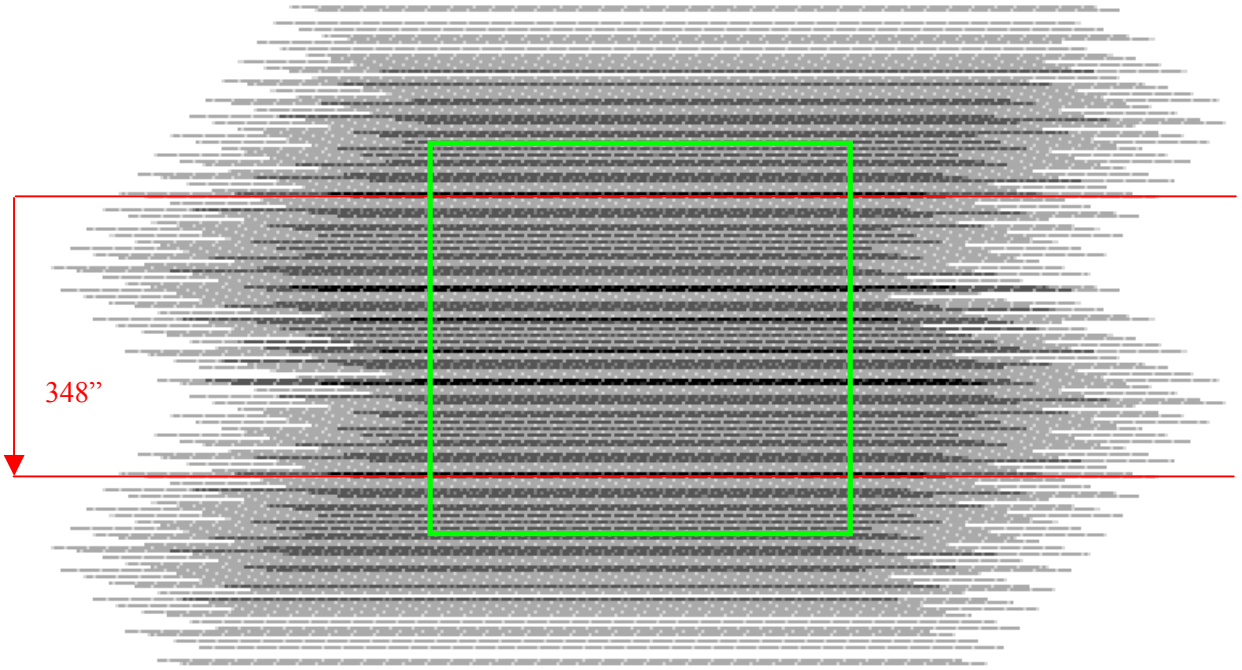

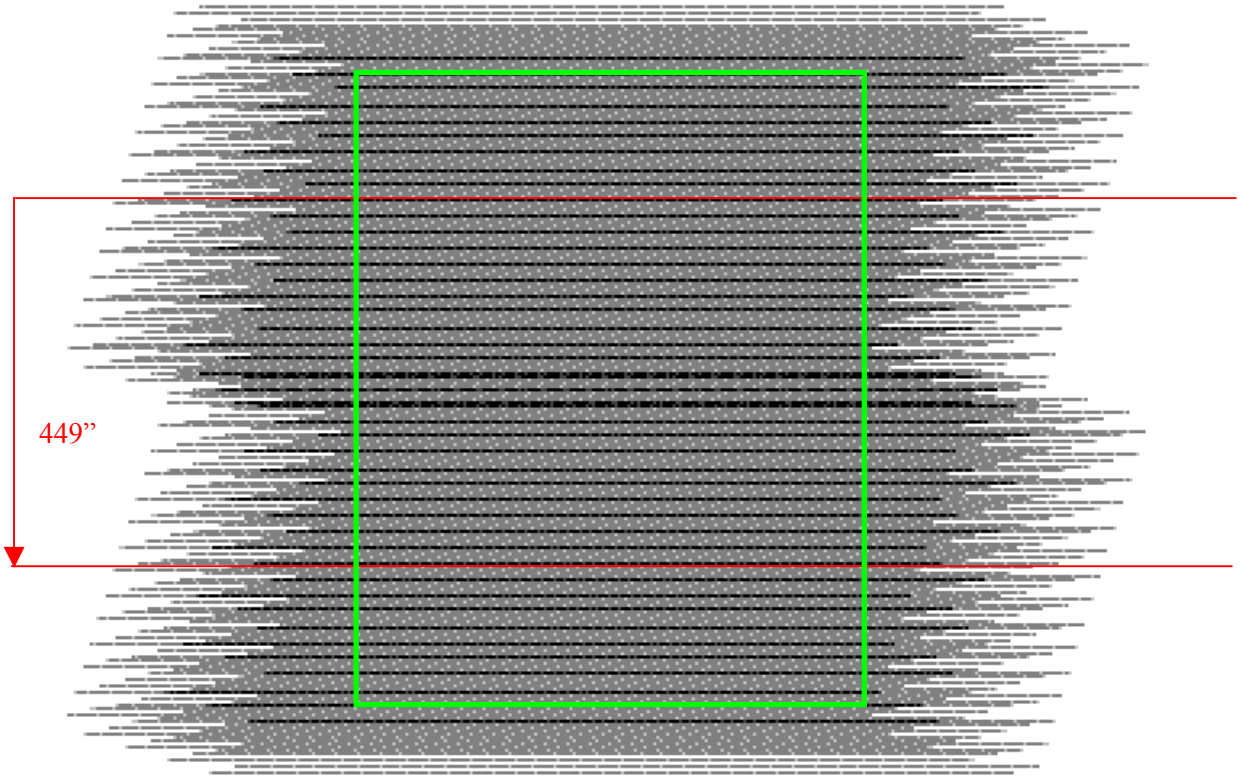

The green boxes give some indication of the map area that contains only the most uniform data coverage. The edges of the map have less integration time because less of the array has passed over those particular areas, and so these edges must fall outside of the area requested by the observer when planning their observation. Essentially we must over-scan the desired map area to ensure we cover it uniformly.

Figure 7. Schematic showing the geometry of the map area covered by a small scan pattern.

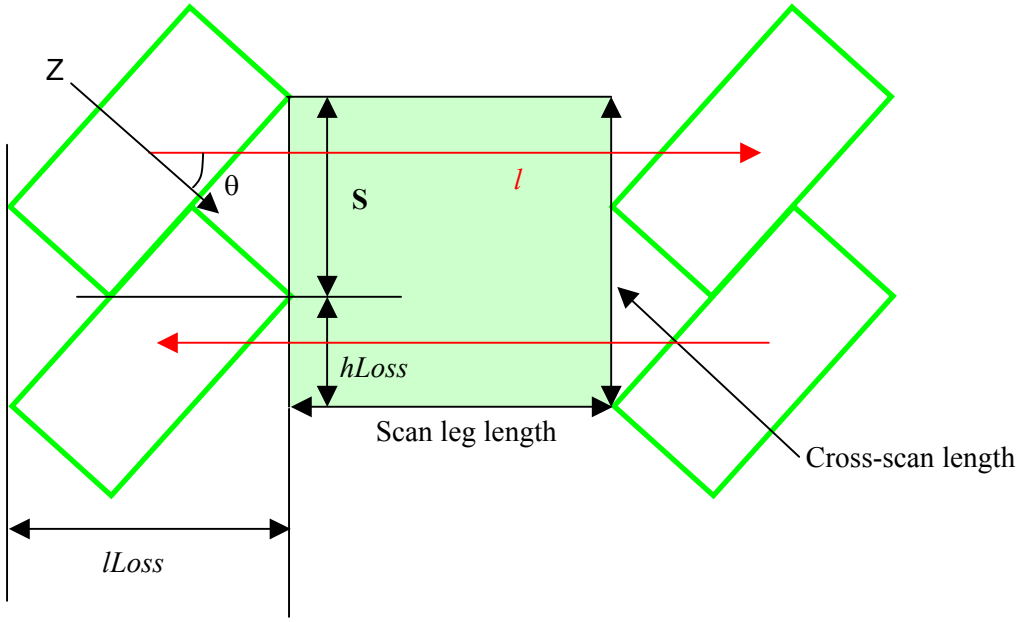

Figure 7 shows how it is possible to calculate the size of a map using geometric arguments, rather than using the integration time maps. The parameters *hLoss* and *lLoss* are CUS parameters designed to ensure the user requested map area is covered properly (*lLoss* is shown in one block here but in reality it will be split in half, with the scan leg starting *lLoss*/2 before the array centre reaches the map edge, and finishing *lLoss*/2 after the map has been passed, as shown by the red lines.) They are related to the scan direction and the size of the

SPIRE arrays, as we shall see. In fact, Figure 7 is simply a zoomed out version of Figure 2 and we shall be using both for this derivation. Refer also to Table 1 for the dimensions of the array rectangles.

$$lLoss = width_{PLW} \cdot \cos(\theta) + height_{PLW} \cdot \sin(\theta) = 561"$$

$$hLoss = \left| height_{PSW} \cdot \cos(\theta) - width_{PSW} \cdot \sin(\theta) \right| = 194"$$

The *lLoss* and *hLoss* parameters are summarised in Table 3. Note how *lLoss* is calculated using the size of the PLW array; it is better to ***overestimate*** *lLoss* than to underestimate it, so the largest array is used here. Also, note how *hLoss* is calculated using the PSW array; it is better to ***underestimate*** *hLoss* than to overestimate it. In this way, the user will always be happy with the size of their map. Finally, note how the *hLoss* parameter is the modulus; the sign flips round for long axis scanning, compared to the other two, because the left and right corners of the array reverse their order from top to bottom (try it out for yourself!)

Table 3. *lLoss* and *hLoss* parameters for the three different scan directions, in arc seconds.

Scan Angle	*lLoss*	*hLoss*
long	580	134
diagonal	561	194
short	421	390

The cross-scan length of a map is related to the number of scan legs, the separation between them, and *hLoss*. This is given by the numbers in Table 4, where n = number of scan legs, and the separations and *hLoss* are indicated explicitly.

Table 4. Calculation of cross-scan length from the number of scan legs.

Scan Angle	~cross-scan length
long	235"*(n-1)+134"
diagonal	348"*(n-1)+194"
short	449"*(n-1)+390"

The scan leg length of the map is related to the length of the scan line performed at uniform scan speed. Table 5 summarises this distance for each scan angle, where l = total length of uniform speed scan leg in arc seconds and *lLoss* is indicated explicitly.

Table 5. Calculation of scan leg length from the distance actually traversed by the arrays while travelling at the constant scan speed.

Scan Angle	~scan leg length
long	l-580"
diagonal	l-561"
short	l-421"

To calculate the number of scan legs required, given a requested cross-scan length, the formulae in Table 4 need to be inverted and n rounded up to the nearest integer.

e.g. user required cross-scan length = 12 arc min, diagonal scanning.

n = roundup[(12*60 – *hLoss*)/*scan_leg_sep*] + 1

$\Rightarrow$ n = roundup[(12*60 – 194)/348] + 1 = 3

Note the negative in front of the *hLoss*. Putting a zero height map returns a value of n = 1, as it should be.

To calculate the distance that the arrays need to travel in the scan leg direction, given a scan leg length, the formulae in Table 5 need to be inverted.

e.g. user required scan leg length = 12 arc min, diagonal scanning.

$l = (12*60) + lLoss$

$\Rightarrow \quad l = (12*60) + 561 = 1281" = 21.35'$

These dimensions do not take cross linked observations in to account – the map area becomes slightly non-square (or non-rectangular) due to the orthogonal scanning direction being 84.8° (or 95.2° depending on your point of view) rather than 90°. If two square (or rectangular) orthogonal maps are combined the circular guaranteed area remains the same however (see Figure 8), so these numbers should still be used for the basis of planning observations.

Figure 8. Combining two rectangular 'orthogonal' scan map observations results in a slightly non-rectangular map, shown by the bright green area, but the guaranteed area, shown by the dark green inner circle, remains unchanged.

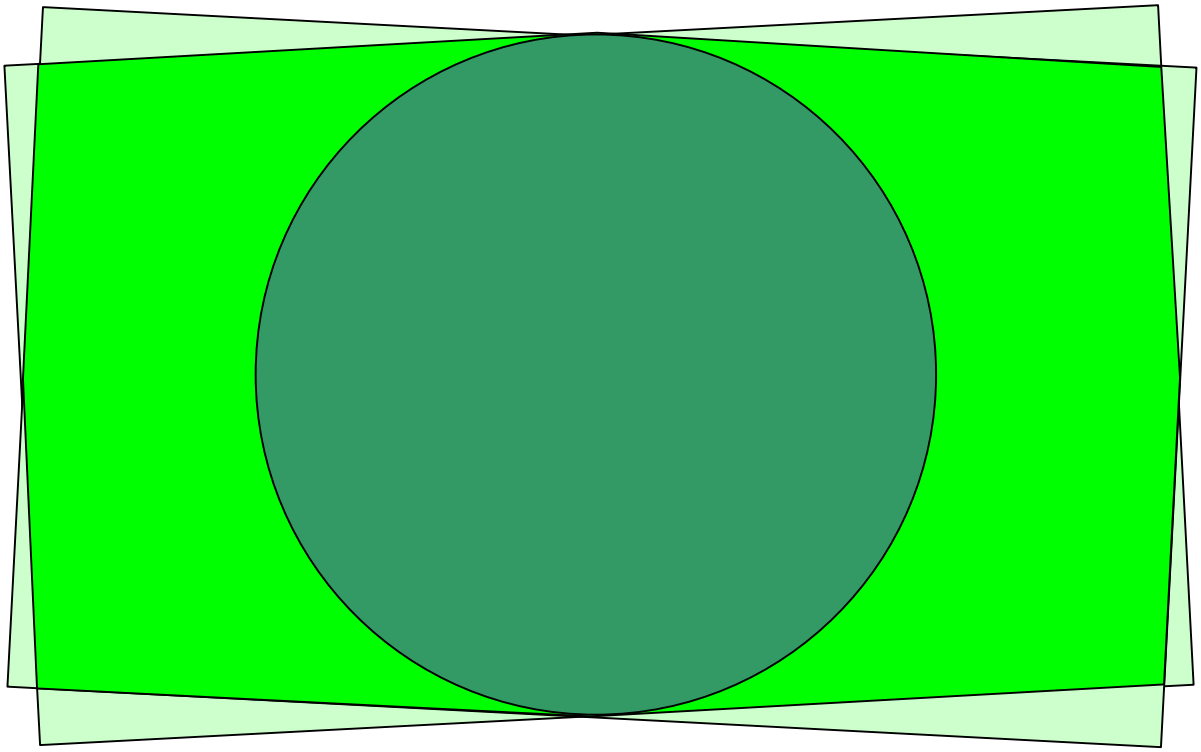

8.1 hLoss and lLoss for pMode

pMode follows the diagonal scan direction but uses a scan leg separation of 155" rather than the 348" that the equivalent SPIRE only scan direction uses.

Figure 9 demonstrates how the reduction in **S** leads to a complete change in the assumptions needed to calculate the size of the SPIRE map. *lLoss* will be the same as with SPIRE only, since the size of the map in the scan leg direction is not affected by the different value of **S**. ***hLoss* is now negative, however**, and now three scan legs are required to get a strip of uniform data. As before:

$$-hLoss_p = height_{PSW} \cdot \cos(\theta) - width_{PSW} \cdot \sin(\theta) = 194"$$

This is the same value as *hLoss* was before but now it must be subtracted from the map size rather than added on. The size of the uniformly covered map area in the cross-scan direction is now:

$$cross\_scan\_length = 155"(n-1) - 194"$$

where n is the number of scan lines.

By inverting this we obtain an expression for the number of scan legs given the required cross-scan length of the map.

e.g. user required cross-scan length (for the SPIRE part of the pMode map) = 12 arc min.

n = roundup[(12*60 – $hLoss_P$)/$scan\_leg\_sep$] + 1

$\Rightarrow$ n = roundup[(12*60 + 194)/155] + 1 = 7

Following this logic it is easy to see why three is the minimum possible value for n. For a map with zero cross-scan length: 194/155 + 1 = 2.25, round up to the nearest integer = 3.

Figure 9. Schematic showing how pMode affects the SPIRE scan map geometry.

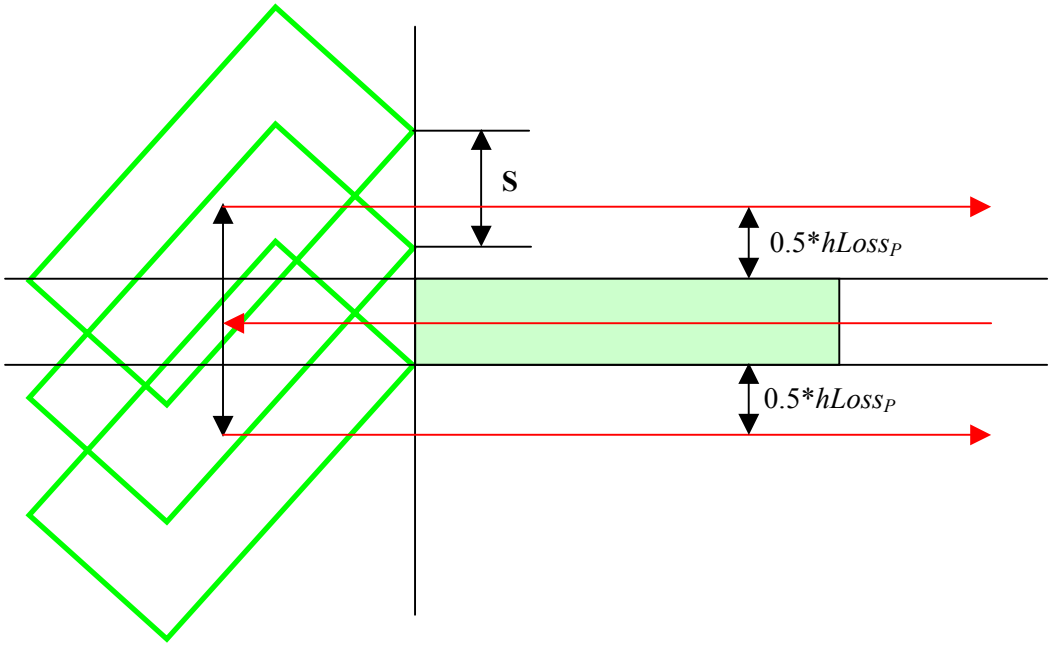

Figure 10. By shifting the array footprints to either side it is clearer how three scan legs are necessary before a uniform coverage region is produced.

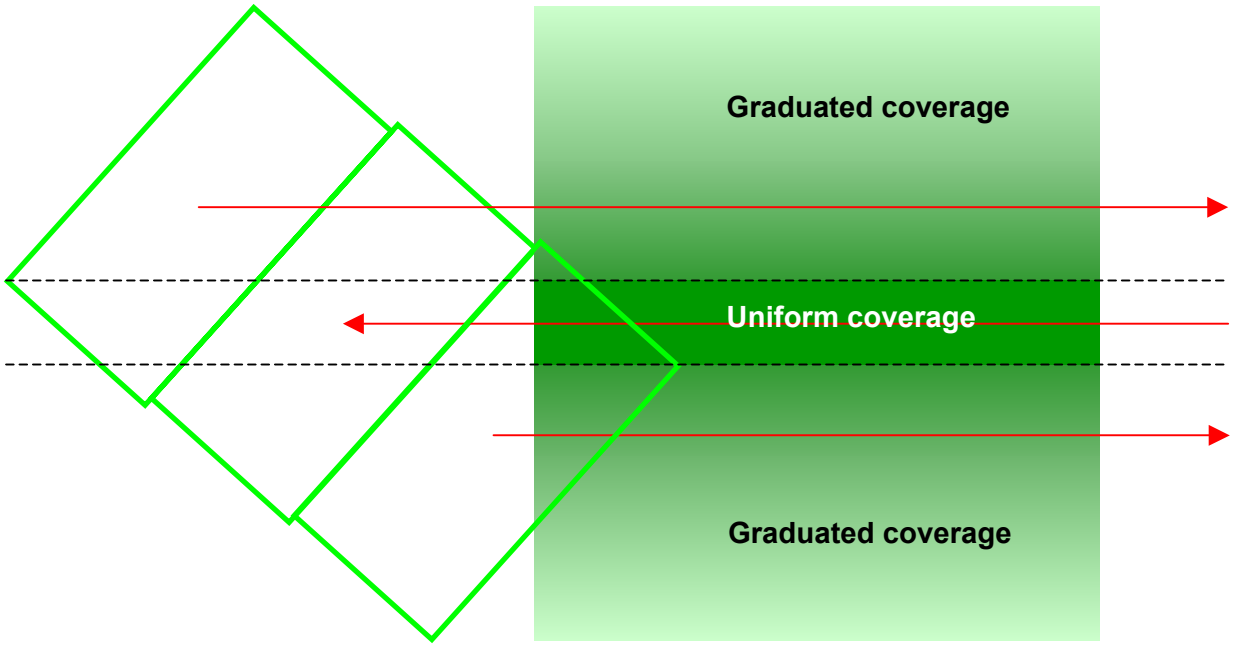

Showing Figure 9 in a slightly different way gives us Figure 10. Here the top array footprint has been shifted to the left while the bottom array footprint has been shifted to the right. This expanded view shows how the coverage map is built up, since the effective integration time across the coverage map is now proportional to the horizontal cross-section through the three array footprints, combined together. Only the central section, bounded by the vertical position of the far left and right corners, has a constant horizontal cross-section, and hence uniform coverage. Three scan legs are necessary to achieve any uniform coverage area at all.

Well, this is what the situation would be like if we didn't have to worry about PACS. Unfortunately things get complicated now because PACS and SPIRE are separated somewhat in the Herschel FoV.

Figure 11 shows what happens to the scan pattern when we add PACS into the mix. The SPIRE and PACS FoV centres are 21 arc minutes apart along the Z-axis. Therefore the extra *lLoss* that's required is made up as follows: 21*60*cos(42.4) – 0.5**lLoss(SPIRE)* + 0.5**lLoss(PACS)*.

21*60*cos(42.4) is the horizontal distance between the SPIRE and PACS FoV centres

0.5**lLoss(PACS)* is the extra half of the PACS FoV that must be taken into account to ensure that PACS completely covers the requested area.

-0.5**lLoss(SPIRE)* is required because the extra *lLoss* starts at the corner of the SPIRE FoV and not at the SPIRE center.

The total *lLoss* required for pMode is the standard *lLoss* described earlier plus this extra *lLoss*.

i.e. $lLoss_P = 21 \cdot 60 \cdot \cos(42.4) + 0.5 \cdot 561 + 60 \cdot 0.5 \cdot \left(3.5 \cdot \sin(42.4) + 1.75 \cdot \cos(42.4)\right) = 1321''$

The last part is the calculation of the PACS equivalent of *lLoss* based on the fact that the PACS FoV is 3.5 x 1.75 arc minutes.

Extra *hLoss* is also needed and this can be calculated by looking at Figure 11 again. The vertical distance between the SPIRE and PACS FoV is simply 21*60*sin(42.4) but we need to subtract a small amount to account for the top right corner of the PACS FoV being above the PACS centre.

The total *hLoss* is then calculated by adding on half of the *hLoss* calculated above, i.e. the bottom 0.5**hLoss*$_P$ in Figure 9.

i.e.

$$-hLoss_P =$$

$$60 \cdot 21 \cdot \sin(42.4) - [60 \cdot 0.5 \cdot (3.5\cos(42.4) + 1.75\sin(42.4)) - 1.75\cos(42.4)] + 0.5 \cdot 194 = 911''$$

The 0.5**hLoss*$_P$ at the bottom of Figure 11 is the same as the 0.5**hLoss*$_P$ at the bottom of Figure 9 – because of the necessity of having that last scan leg, to ensure that the bottom of the map is covered uniformly – so this total *hLoss*$_P$ amounts to 5 extra scans before the start of the user requested map area, and one afterwards.

Figure 11. Schematic showing how the SPIRE and PACS FoV fit together, and how this leads to extra *hLoss* and *lLoss* being required to ensure that both instruments fully cover the user requested area (shown again here as the green rectangle.)

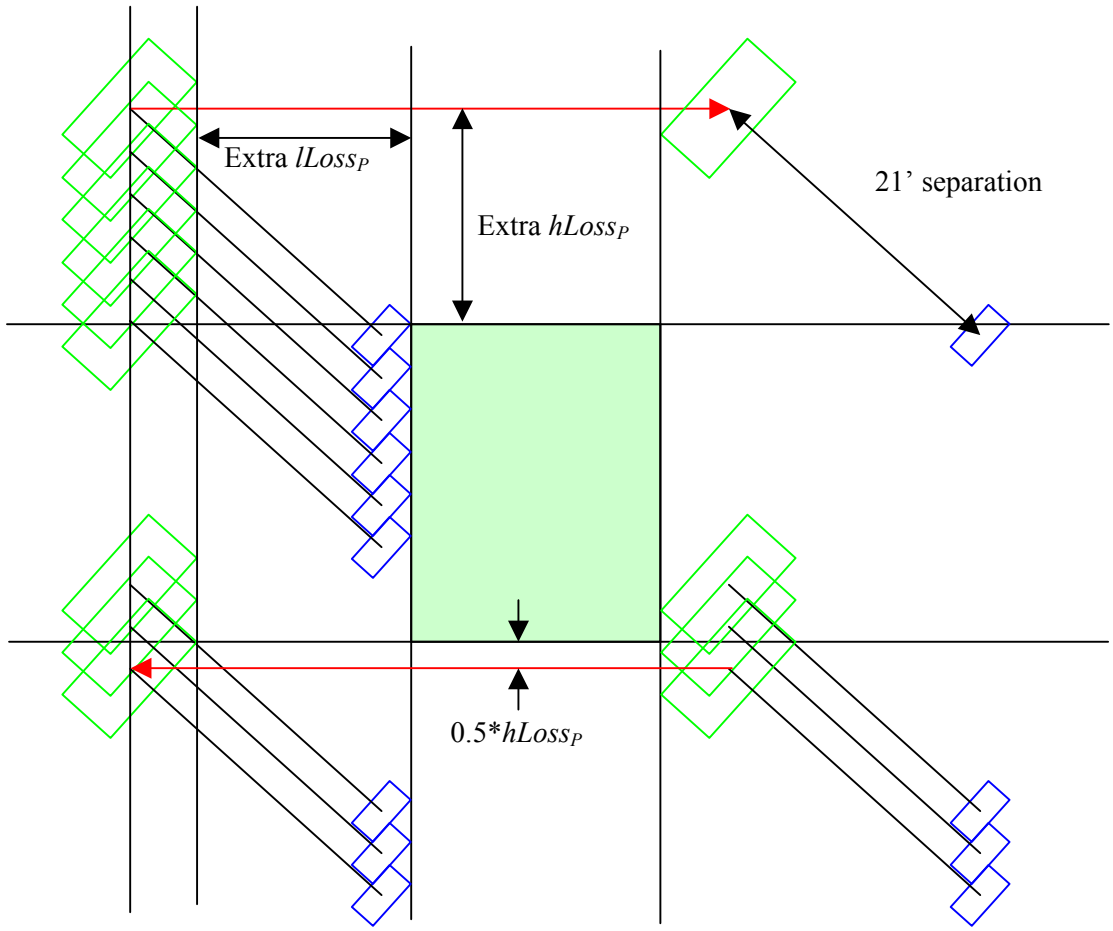

Importantly, and in contrast to SPIRE only mode, it is now better to ***overestimate*** both $lLoss_P$ and $hLoss_P$, (or rather the absolute value of these parameters should be overestimated) because both now account for extra space outside of the boundary marked out by the requested map, rather than the map extending beyond the area defined by the path of the SPIRE array centre, as with *hLoss* for SPIRE only. **Essentially this boils down to the fact that *hLoss* now has a negative sense compared to the SPIRE only value, and so the value in the calibration table must be negative.**

These numbers are summarised in Table 6.

Table 6. $lLoss_P$ and $hLoss_P$, for parallel mode, in arc seconds.

Scan Angle	$lLoss_P$	$hLoss_P$
long	?	?
diagonal	1321	– 911
short	?	?

The minimum number of scan legs is clearly more than 3 now. For a map of zero cross-scan length we now have:

$$n = \text{roundup}[(0*60 - hLoss_P)/scan\_leg\_sep] + 1$$
$$\Rightarrow \quad n = \text{roundup}[(0*60 + 911)/155] + 1 = 7$$

Although, in reality the minimum size of a parallel mode map is 30 arc minutes square, so the minimum number of scans would actually be:

$$n = \text{roundup}[(30*60 - hLoss_P)/scan\_leg\_sep] + 1$$
$$\Rightarrow \quad n = \text{roundup}[(30*60 + 911)/155] + 1 = 19$$

This logic is exactly the same as for SPIRE only, as long as the $hLoss_P$ parameter is correct in the calibration table.

9. References

[1] *SPIRE Photometer Simulator Verification – Scan Map Sensitivity,* Tim Waskett, Bruce Sibthorpe, SPIRE-UCF-NOT-002756
[2] *Cross Linked Scan Map Observations,* Tim Waskett, Bruce Sibthorpe, SPIRE-UCF-NOT-002759
[3] *Scan Map Scanning Angles and Separations*, Tim Waskett, Bruce Sibthorpe, SPIRE-UCF-NOT-002758